Advanced Horizontal Well Recirculation Systems for Geothermal Energy Recovery in Sedimentary Formations

M.S. Bruno, V. Serajian, K. Lao, and A. White
Terralog Technologies USA, Inc.

Jean E. Elkhoury & Russell L. Detwiler
Dept. of Civil & Environmental Eng., University of California, Irvine

Keywords: Horizontal wells, Sedimentary formations, Geothermal energy, Recirculation systems

1. Abstract

There is increased recognition that geothermal energy resources are more widespread than previously thought, with potential for providing a significant amount of sustainable clean energy worldwide. Recent advances in drilling, completion, and production technology from the oil and gas industry can now be applied to unlock vast new geothermal resources, with some estimates for potential electricity generation from geothermal energy now on the order of 2 million megawatts.

Terralog USA, in collaboration with the University of California, Irvine (UCI), are currently investigating advanced design concepts for paired horizontal well recirculation systems, optimally configured for geothermal energy recovery in permeable sedimentary and crystalline formations of varying structure and material properties. This two-year research project, funded by the US Department of Energy, includes combined efforts for: 1) Resource characterization; 2) Small and large scale laboratory investigations; 3) Numerical simulation at both the laboratory and field scale; and 4) Engineering feasibility studies and economic evaluations. The research project is currently in its early stages. This paper summarizes our technical approach and preliminary findings related to potential resources, small-scale laboratory simulation, and supporting numerical simulation efforts.

2. Application of Horizontal Wells to Geothermal Energy Recovery in Hot Sedimentary Rock

Horizontal well technology has advanced rapidly in the past 10 years, allowing new economic production from both conventional and unconventional resources (including shale gas developments and heavy oil thermal developments). For thermal enhanced oil recovery in particular, advanced horizontal well pair and multi-well configurations and operating practices have allowed development of significant new heavy oil production through application of steam assisted gravity drainage systems (SAGD), cyclic steam stimulation operations (CSS and "huff and puff") and horizontal assisted steam drive system (HASDRIVE). To date, however, such innovative horizontal well systems and technology have not been widely transferred or applied within the geothermal energy industry. The key impediments have been high well costs (which are declining with improved drilling technology) and limited design optimization and economic studies (as geothermal energy recovery requires different operating practices than thermal stimulation).

Terralog and the University of California, Irvine, are currently investigating advanced design concepts for paired horizontal well recirculation systems, optimally configured for geothermal energy recovery in permeable sedimentary formations of varying structure and material properties.

For example, one technique proposed by Terralog USA involves placing one or more horizontal well pairs (one injector and one producer) to establish a relatively closed loop recirculation system, optimally positioned for maximum heat energy production given the thermal and flow properties for the given formation. Two advantages to this approach include more efficient and controlled flow and heat transfer, and reduced wastewater management requirements.

The primary challenge for such recirculation systems is to optimize both the design configuration and the operating practices for cost-effective geothermal energy recovery. These will be strongly influenced by sedimentary formation properties, including thickness and dip, temperature, thermal conductivity, heat capacity, permeability, and porosity; and by working fluid properties. For example, optimum design configurations and operating practices to be considered include (but are not limited to):

- Separation distance between wells and well pairs;
- Injection length versus production length (perforated intervals);
- Continuous versus cyclic injection and production (heat soak, huff and puff);
- Injection rates versus production rates; and,
- Working fluid properties (including potential use of CO2);

The fundamental concept and method for extracting heat from the subsurface is illustrated schematically in Figure 1. One or more horizontal well pairs (which may be spaced vertically or laterally depending on formation properties) are placed to establish a (relatively) closed loop recirculation system.

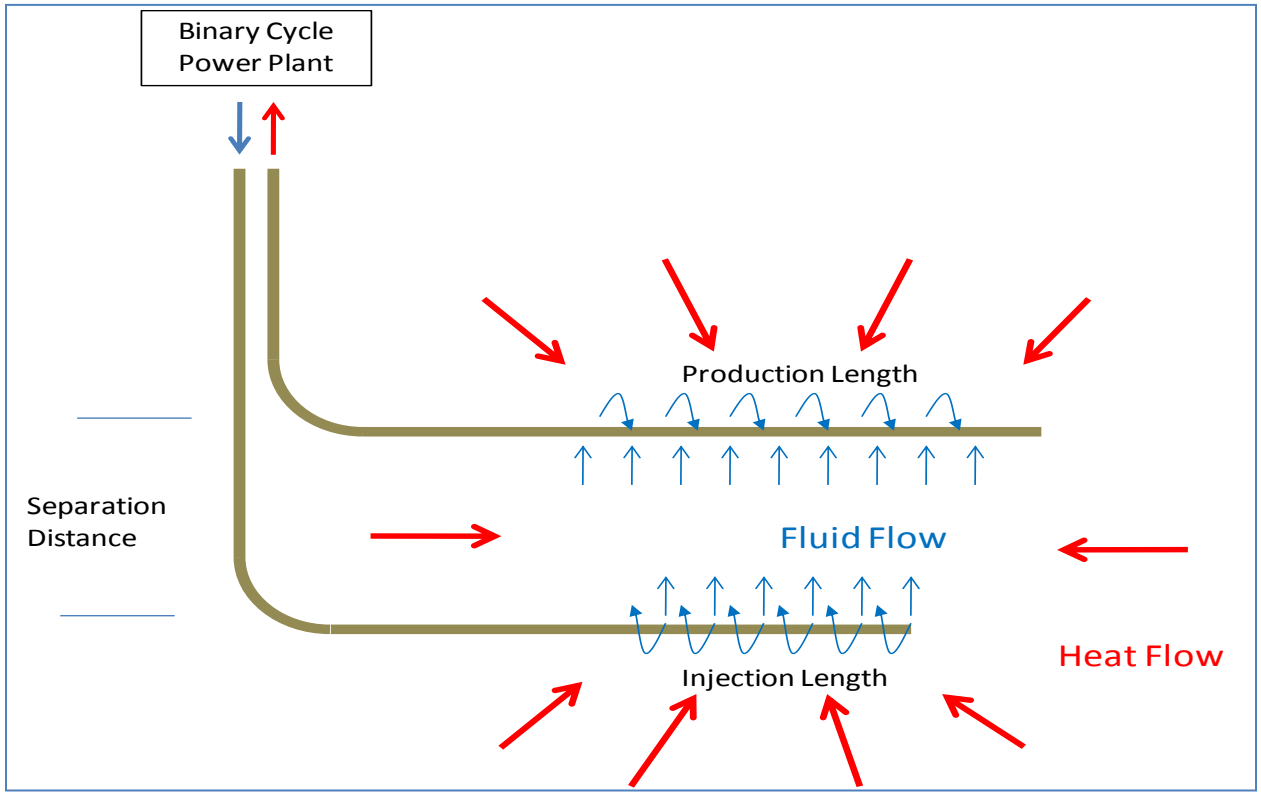

Figure 1: Horizontal well pairs for closed loop geothermal recovery system

Environmental Advantages and Risk Reduction

Application of advanced horizontal well circulation system technology in permeable sedimentary formations may provide a number of significant advantages over traditional geothermal recovery and enhanced geothermal systems in low-permeability crystalline formations. These include:

1.) *Reduced risk for induced seismicity.* Permeable sedimentary rocks are generally less brittle and less seismically active than crystalline rocks. Porous flow through the rock matrix induces much lower stress as compared to fracturing in crystalline formations. Induced microseismicity is lower in magnitude and attenuates more rapidly.

2.) *Reduced need for surface wastewater disposal.* A closed or near closed loop recirculation system reduces the need for surface evaporation ponds or surface discharge of wastewater. Continuous fluid circulation provides better control of fluid chemistry, potentially reducing carbonate and silicate precipitation problems (and the need for scale disposal).

3.) *Potential combination with CO_2 sequestration.* Some researchers have suggested that CO_2 might be a more effective working fluid than water. Lower viscosity provides easier flow for a given pressure gradient. Heat transmission properties are on the same order as water. And CO_2 may reduce scaling problems. If the injection rate is set higher than the production rate in a dual wells system, some of the supercritical CO_2 would operate as the working fluid while the remainder is sequestered in the formation, providing dual benefits.

3. Potential Geothermal Resources in US Sedimentary Basins

There is increased recognition that Geothermal Energy Resources are more widespread than previously thought, with potential for providing a significant amount of sustainable clean energy worldwide (see for example Holbrook et al, 2011; Morgan and Sares, 2011; Porro and Augustine, 2012). Recent advances in drilling, completion, and production technology from the Oil and Gas Industry can now be applied to unlock vast new geothermal resources, with some estimates for potential electricity generation from Geothermal Energy now on the order of 2 million megawatts.

Several sedimentary basins throughout the United States contain stored geothermal energy that can be utilized for electricity production. We have identified eight potential areas within various sedimentary basins that are at accessible depths and reach appropriate temperatures for energy recovery. Our initial focus is on locations and formations that reach an estimated temperature of at least 150°C at depths less than 3.5 km. Some of these regions are identified in Table 1, and are shown in red in Figure 2.

Table 1: Selected regions throughout the U.S. that reach a minimum 100°C at 3.5 km depth or less with corresponding sedimentary basins

Potential and confirmed geothermal resources that reach temperatures greater than 150°C	Sedimentary Basin
1. Salton Trough Area	Imperial Valley Basin
2. Western Idaho	Snake River Basin
3. Central New Mexico	Albuquerque Basin
4. Southern Colorado	Raton Basin
5. Central Colorado	Denver Basin
6. Northeastern Texas	Gulf Coast Basin
7. Northwestern South Dakota	Gulf Coast Basin
8. Eastern West Virginia	Appalachian Basin

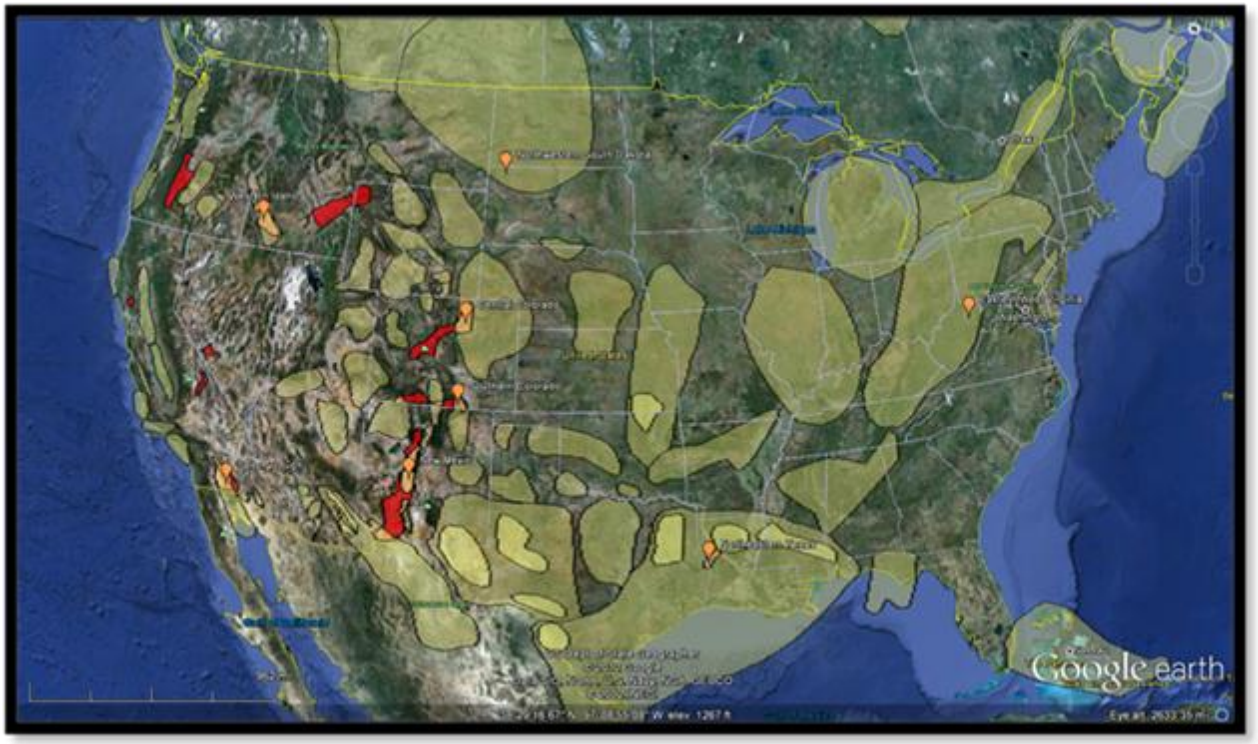

Figure 2: Map of geothermal characterization sites (orange pins) throughout the US. Regions in red indicate areas that reach a minimum of 150°C at ≤ 3.5 km. Sedimentary basins and sub-basins are shown in shading.

4. Preliminary Laboratory Experiments

Our laboratory experiments consist of fluid flow through a heated sedimentary rock while we monitor the pressure gradient and temperature evolution at the inlet and outlet of our system (Figure 3). Our sample is an intact Castlegate sandstone disc of 22.9 cm (9 in) diameter and 3.81 cm (1.5 in) thickness. The sample is heated (temperature controlled) at its circumference by a heating tape (Figure 4). We performed two sets of preliminary experiments with de-aired deionized (DI) water as the pore fluid. The first set consisted of three experiments, labeled Toa, Tob and Toc, run at room temperature and varying confining pressures (Table 2). The second set consisted of four experiments, labeled T1 to T4, where we heated the sample to temperatures up to 75^{o}C (Table 2). The thermocouples measured the temperature as

a function of time at about 1.3 cm (0.5 in) into the rock (Figure 4). The inlet boundary condition was flow controlled and the outlet boundary condition was open to atmosphere (Figure 3). We applied flow rate steps at the inlet between 1 ml/min and 25 ml/min. We used two pumps under continuous flow mode at the inlet providing smooth pressure switching between the pumps. Our experimental sequence was as follows: 1) we waited until the system reached a steady-state temperature under no flow condition; 2) we initiated flow with the lowest flow rate and waited until the inlet and outlet temperatures reached steady-state and then we increased the flow rate; 3) we waited until the inlet and outlet temperatures reached steady-state and again increased the flow rate; 4) we repeated step 3 until we reached the highest flow rate of our sequence.

For the next sequence, we stopped flow, increased the temperature and waited for steady-state temperature and repeated the sequence of flow rate steps described in items 2 and 3 above. This particular sequence means that we did not reheat the sample or waited for the temperature to recover to its pre-flow value after each flow step. However, we did run one experiment, T4, to specifically test the influence of reheating the sample after each flow rate step.

4.1 Room Temperature Experiments

Figure 5 shows the relationship between the flow rate, Q, and the pressure difference, ΔP, for a range of flow rates at room temperature. For each confining pressure, P_c, we started with the flow rate of 2 ml/min and increased it up to 25 ml/min. Here, we highlight two main observations: 1) the overlapping of the data for different confining pressures and 2) the linear relation between ΔP and Q (0.083 psi/(ml/min)) that provides a robust estimate of the permeability of our Castlegate sample (1140 mD) obtained from our numerical simulation presented in Section 6 (dashed line in Figure 5). It also provides a working range of flow rates for this preliminary stage in our experimental investigations[1].

4.2 Higher Temperatures

We performed three experiments, T1, T2 and T3 at 37.5^{o}C, 67.0^{o}C and 74.9^{o}C set temperatures respectively. As expected, the steady-state temperatures decrease with increasing flow rate and the decrease is greater at the inlet (Figure 6). Also, the steady-state temperatures do not depend on the initial starting temperatures as shown by the overlap of the data from T1 and T4 (Figure 6). Figures 7a, 7b and 7c show the evolution of temperature as we apply flow rate steps at the inlet. For each flow rate step (vertical dashed lines in Figure 7), the temperature decreased until it reached steady state. In a forth experiment (T4), at 37.5^{o}C set temperature, we allowed the system to recover to the pre-flow temperature before applying each flow-rate step (Figure 7d). The temperature difference between the outflow and room temperature decreases with increasing flow rate, as expected (Figure 8a). However, the difference between the inflow and outflow temperature is constant for flow rates above 10 ml/min (Figure 8b).

4.3 Resolved Technical Difficulties

Our preliminary temperature measurements showed some biases that we describe in this section. We observed a temperature difference of less than 3% between the inlet and outlet ports at no flow condition (Figure 6 and dashed and dotted lines in Figure 7). This points at a non-isotropic heating of our system

[1] The current length of our manometers (~ 2 m) limits the pressure differential to less than 2.8 psi. However, in subsequent experiments, the limit will be 20 psi given by a low-pressure differential transducer. For higher-pressure differential, we will use the absolute inlet and outlet pressures given by the pump transducers up to 4000 psi.

although negligible. The second observation is that the measured initial temperature at the inlet, T_o, is lower than the set temperature (comparing Table 2 and Figure 6). For example, the set temperature of experiment T3 is 74.9°C, but the initial measured temperature at the inlet is 80.8°C. This difference is due to radiative heat loss from the vessel and the steep temperature gradient between the rock sample and the thermocouple monitoring the heating tape for input to the temperature controller. Another observation is the decrease of the set temperature measured by the temperature controller at the highest T_o and flow rates. We have overcome all these issues in subsequent experiments by using improved thermal insulation of our vessel system and a better control on the temperature of the flow into the vessel. Additionally, we have installed a differential pressure transducer that will continuously monitor the pressure gradient driving the flow. Finally, we have also added an additional thermocouple to continuously monitor the temperature of the confining fluid and the heating tape.

Table 2: Flow rates, Q, set temperatures, T_o, and confining pressures, P_c, for the two sets of preliminary experiments. The first set consisted of flow through the sample at room temperature that provided a robust estimate of the sample permeability. The second set consisted of four experiments at temperatures below 100°C where we observe the heat transfer from the sedimentary rock sample to the fluid as reported in figures 6, 7, 8 and 9.

Experiment	Q [ml/min]	T_o [°C]	P_c [psi]
Toa	2, 5, 10, 20	21.0	50
Tob	2, 5, 10, 15, 20	21.0	25
Toc	2, 5, 10, 15, 20, 25	21.0	10
T1	2, 5, 10, 15, 20, 25	37.5	10
T2	2, 5, 10, 15, 20, 25	67.0	10
T3	2, 5, 10, 15, 20, 25	74.9	10
T4	2, 5, 10, 15	37.5	10

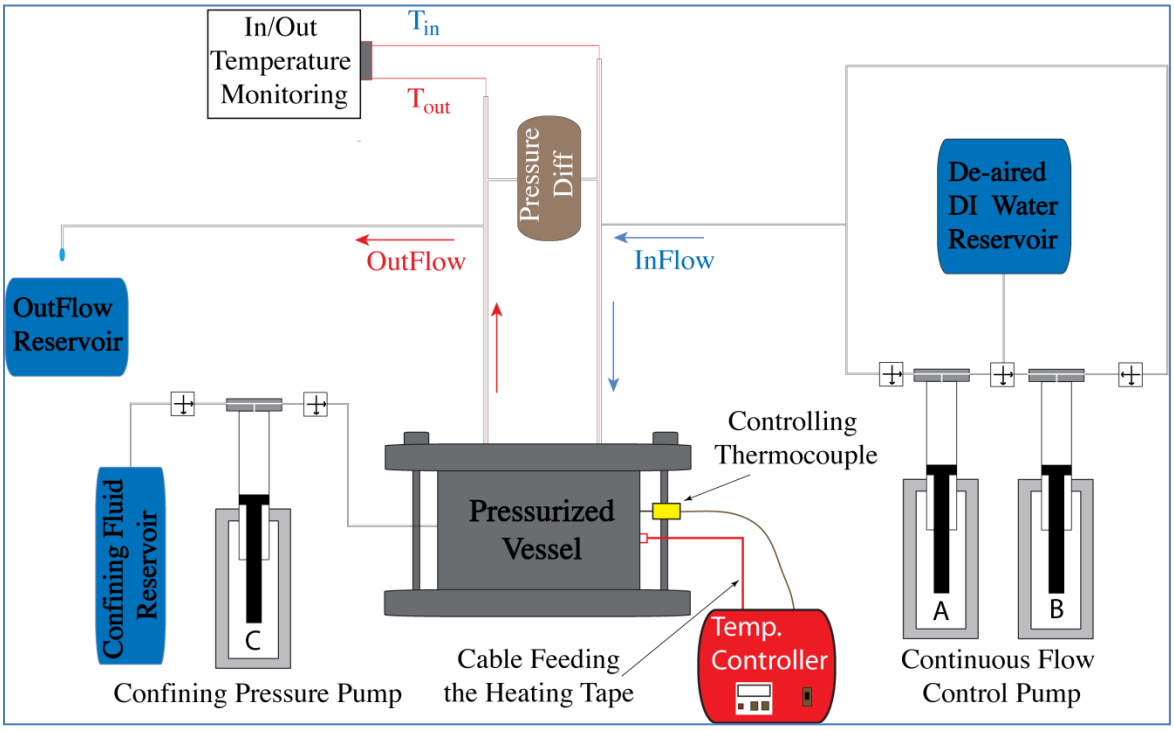

Figure 3: Schematic diagram of our experimental setting. Our sample is pressurized in the vessel where pump C controls the confining pressure. Flow is controlled at the inlet where pumps A and B provide continuous flow and the outlet is open to atmosphere. Inlet and outlet temperatures and pressures are continuously monitored. Sample temperature is monitored and controlled by a temperature controller (red box).

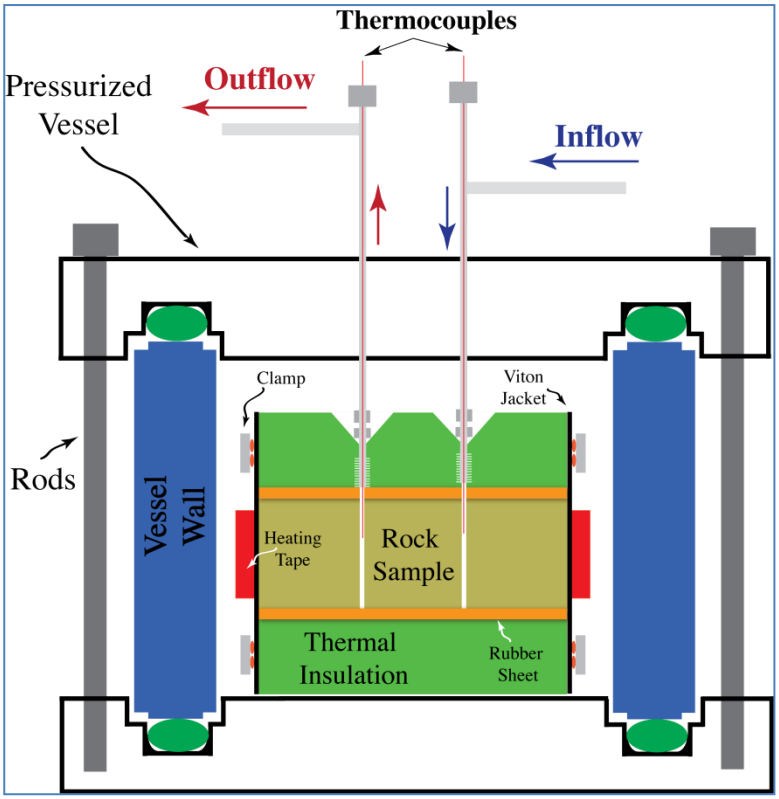

Figure 4: Schematic of a cross section of the sample assembly. The sample has a 9" diameter and is 1.5" thick. Two 1/4" holes, 3" apart and 3" from the edges, were drilled through the sample. The assembly consists of one 1/16" rubber sheet (orange) and a 1" thick Teflon slab (green) on each side of the sample (brown). The o-ring, the Viton jacket and the clamp provide good seal to the assembly. A 1" wide heating tape surrounds the sample providing the necessary heat to keep the sample at a constant temperature. Two thermocouples penetrate the sample about 0.5" to measure the inflow and outflow fluid temperature.

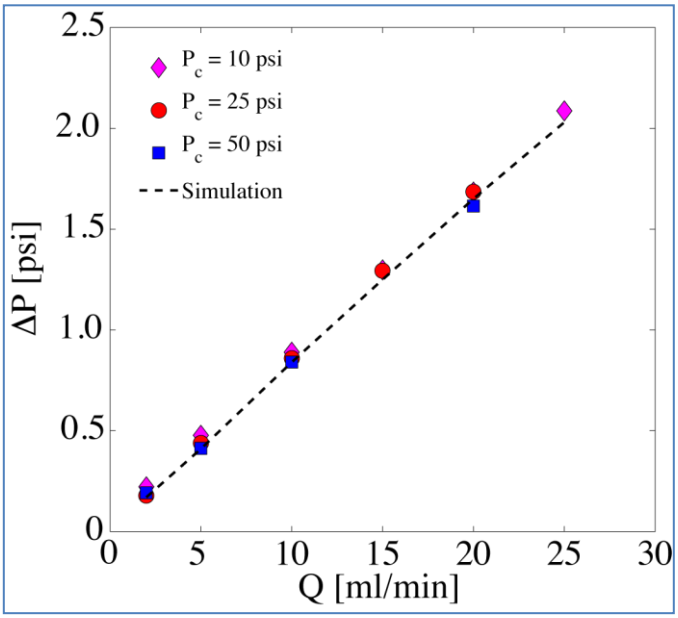

Figure 5: Measured pressure difference, ΔP, between the inlet and outlet of the Castlegate sample at room temperature (~21°C) subject to flow rate, Q, steps. For each P_c, we start with the smallest Q and increase it up to 25 ml/min. Here we highlight two main observations: 1) the linear relation between ΔP and Q, and 2) the overlapping of the data for different confining pressures. Dashed line is obtained from numerical simulations discussed in Section 6 and it corresponds to a permeability of 1140 mD.

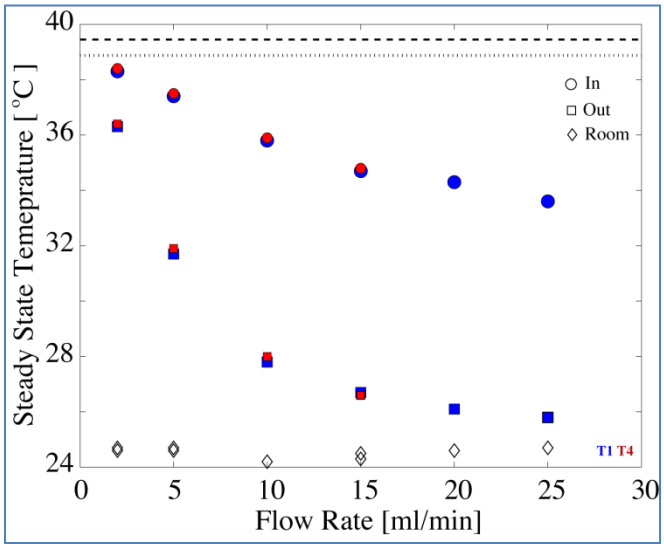

Figure 6: Inlet (square) and outlet (circles) steady-state temperatures from experiments T1 (blue) and T4 (red) as a function of the flow rate steps. Open black diamonds are mean room temperatures during the applied flow rate steps. The horizontal dashed line and the dotted line correspond to the inlet and outlet steady state temperatures during no flow. They provide the initial temperature of our heated system.

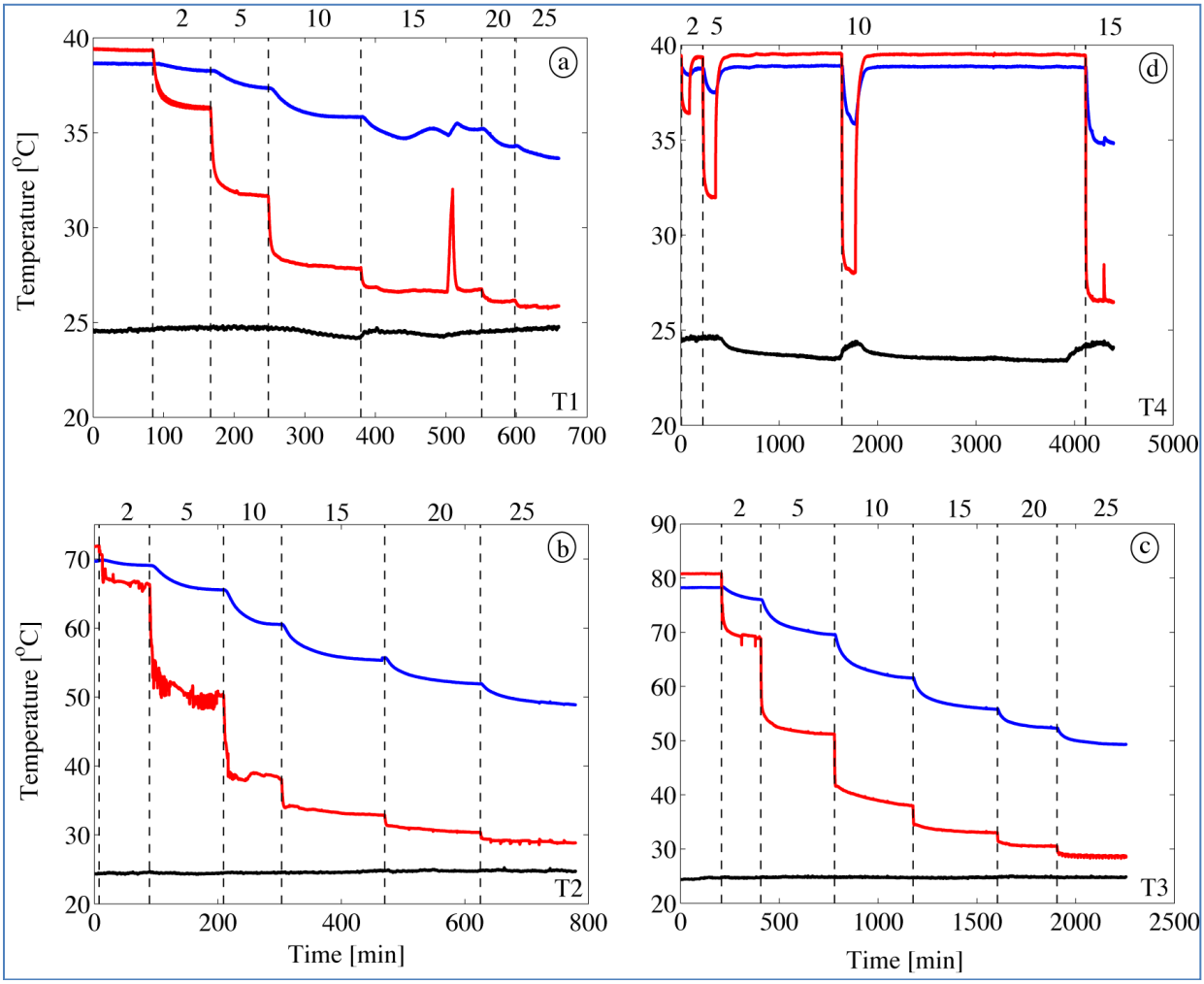

Figure 7: Temperature evolution of the room temperature (black) and the inlet (red) and outlet (blue) temperatures for experiment T1 (a), T2 (b), T3 (c) and T4 (d). Vertical dashed lines correspond to the time at which we applied the flow rate steps. Numbers above the dashed lines are flow rates in units of ml/min. The spike in the outlet temperature around time 500 min for T1 corresponds to the stopping and reinitiating flow through the system. Therefore, the increase in temperature and subsequent decrease, once flow was resumed, are clearly observed. The temperature perturbation in the outlet around the same time is consistent with heating under no flow condition. T3 showed an additional complication compared to previous experiments since the boundary condition changed as the flow rate increased. Boundary condition refers to the constant temperature surrounding the rock sample. As the temperature was not the same for all flow rates. This is resolved by properly insulating the vessel. For T4 we waited for the sample to reheat before applying each flow rate step. The spike in the inlet temperature around 4250 min corresponds to refilling of the manometers which reduced the flow through the sample hence increasing the temperature. The temperature recovers after the manometers stabilized. The effect of this signal is also observed in the outlet temperature profile.

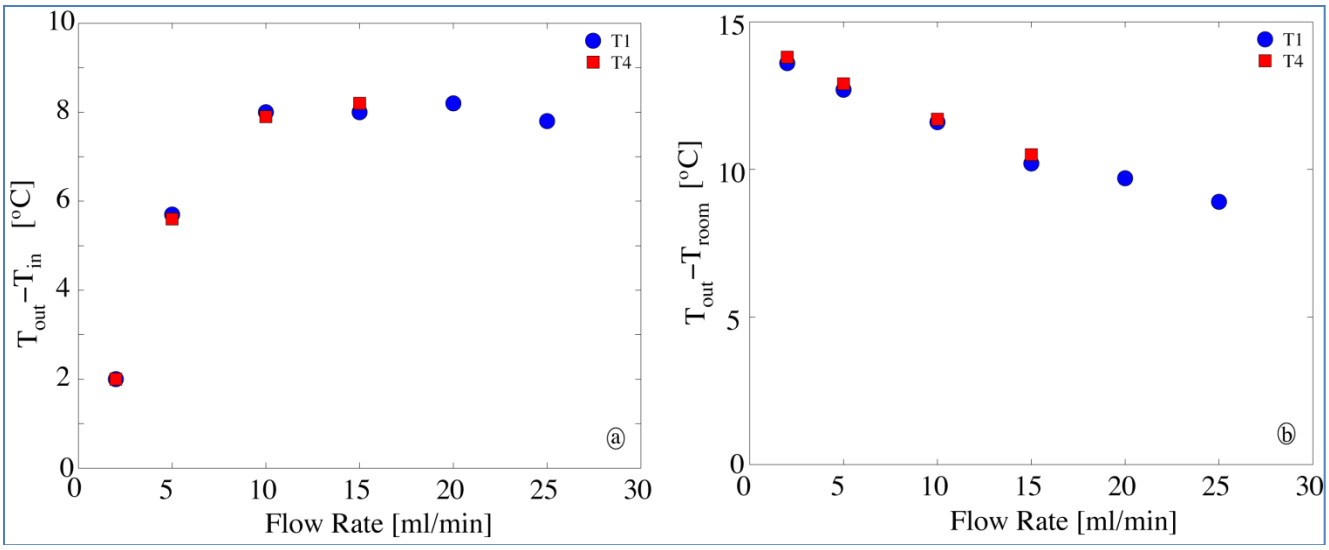

Figure 8: Steady-state temperature difference between the outlet and inlet temperatures (a) and the outlet and room temperatures (b) for experiments T1 (blue) and T4 (red) as a function of the flow rate steps. Notice the overlap between the data set as further evidence for the independence of the steady-state temperature to the initial temperatures, T_o, prior to each flow rate step.

5. Numerical Simulation of Laboratory Experiments

Terralog has developed numerical models of the lab experiments using TOUGH2 software (Pruess et al, 1999). The geometry and initial and boundary conditions are defined consistent with the laboratory configuration. A 3D cylindrical mesh, containing 18,000 grid elements, is defined with a 9 in. diameter, 1.5 in. thick. An injection and production well are placed 3in apart in the center of the slab. Initial material properties estimates for Castlegate sandstone are applied as default parameters, as summarized in Table 3. Parameters are then varied sequentially to observe the variations in the production energy.

Table 3. Physical properties of Castlegate sandstone and the surrounding metal, used in numerical model.

Material	Density (kg/m3)	Permeability (mD)	Porosity (fraction)	Wet Heat Conductivity (W/m/C)	Specific Heat (J/kg/C)
Castlegate Sandstone	2.6 x10^4	750	0.28	2.0	1000

Initial conditions of 100°C and 24.7 psia are applied throughout the model as the initial temperature and pressure, respectively. The injector water temperature is 23 °C and the producer pressure is set to be constant at 24.7 psia. The boundary temperature is set at 100°C. The productivity index (PI), defined as the production volume per unit pressure change ($PI = \frac{\Delta Q}{\Delta P}$) was calculated assuming 100 cc/min water production.

5.1 Simulation Results and Sensitivity Analysis

The results of the temperature changes in the model are presented in Figure 9. Shortly after cold (23°C) water injection starts, the temperature decreases in the model beginning from injection point and spreads in the model gradually. The temperature on the boundaries is still 100 °C since the surrounding metal applies a constant temperature of 100°c from sides of the model. There is almost no difference between figure C and D, indicating that the system has reached steady state flow. The results of the pressure vs.

time variations in the model are presented in Figure 10. The production cell pressure is kept constant at 24.7 psia ($1.7x10^5$ Pa) and as the injection proceeds, the injection pressure increases.

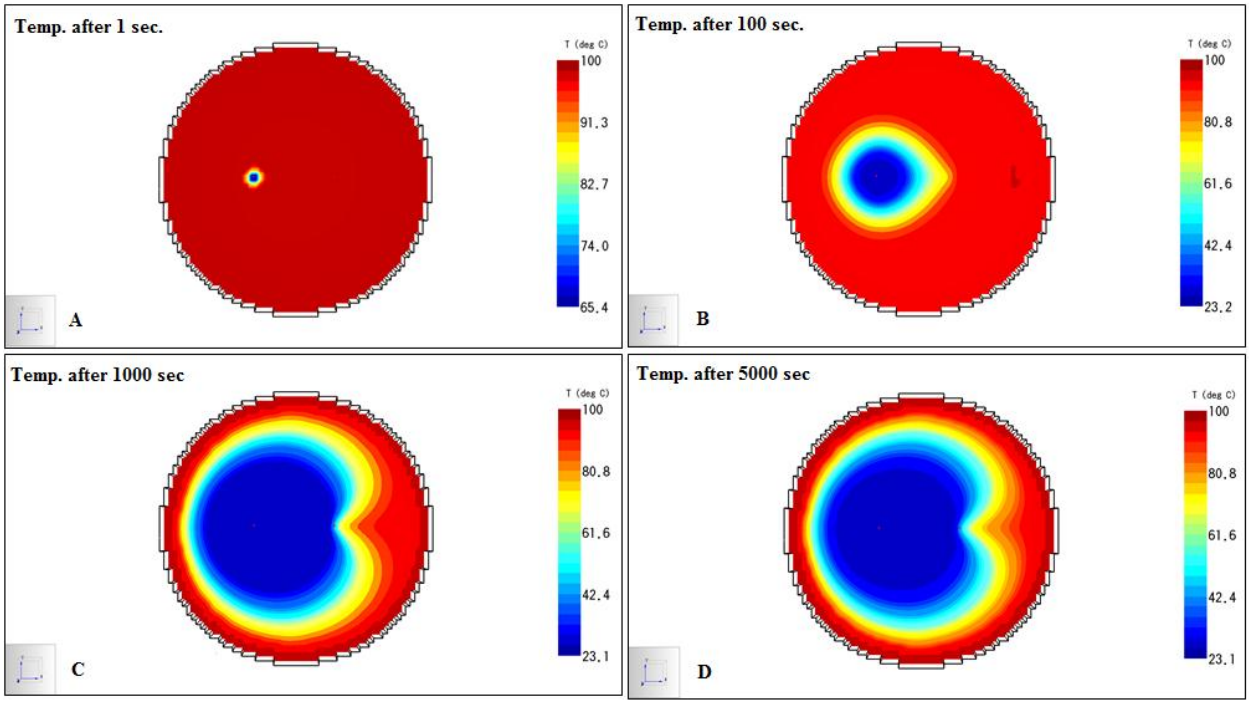

Figure 9. Numerical simulation of temperature distribution in rock sample after cold water injection. As shown in A, immediately after injection start the temperature of the injector decreases rapidly (to about 65°C). The temperature distributions in rock sample are plotted at 100 seconds (B), 1000 seconds (C) and 5000 seconds (D) after cold water injection started. Note that in all cases, rock temperature on the boundary is constant (100°C).

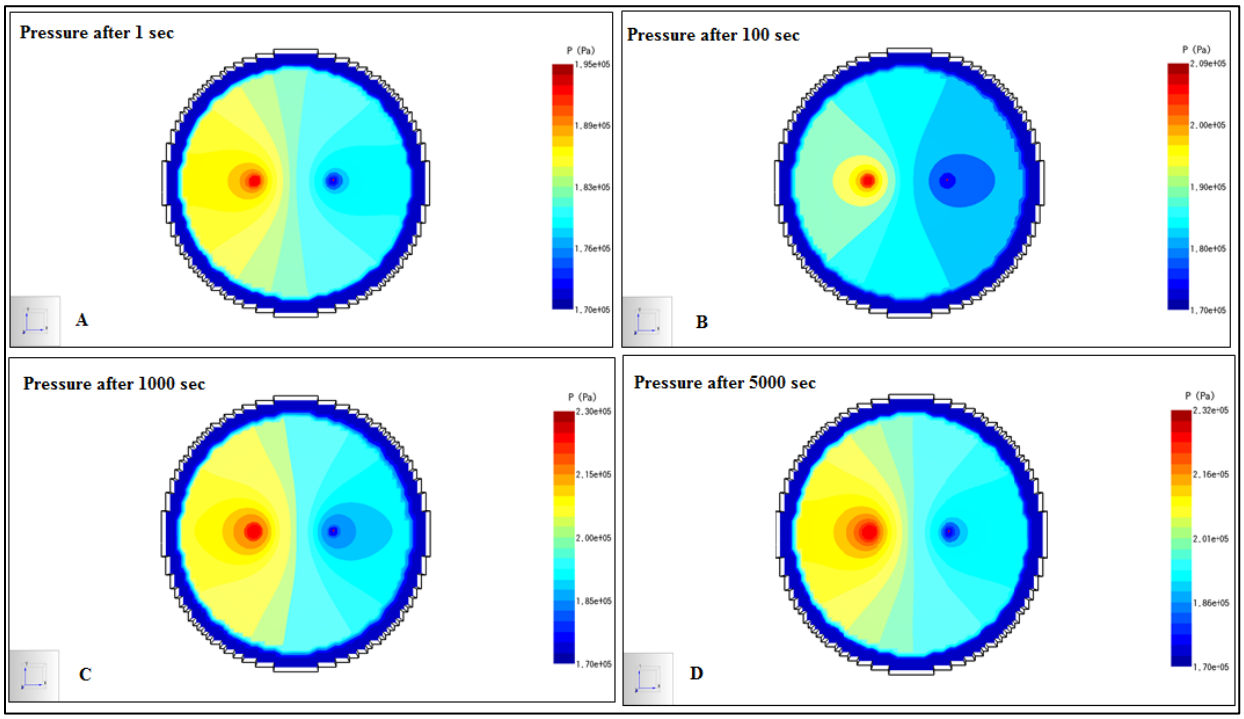

Figure 10. Pressure distribution in the model after 1, 100, 1000 and 5000 seconds following cold water injection. The production pressure is set to be constant ($1.7x10^5$ Pa=24.7 psi) in all four figures (A-D) but the injection pressure increases with time from $1.95x10^5$ Pa (28.3 psi) after 1 second to $2.32 x10^5$ Pa (33.3 psi) after 5000 seconds.

Sensitivity Analysis Results

Terralog carried out a sensitivity analysis on five major parameters which influence the temperature of the produced water. The goal is to identify the most important parameters which influence thermal energy recovery. In this study five different parameters have been varied: 1) Injection rate; 2) Rock permeability; 3) Rock Porosity; 4) Rock specific heat; and 5) Rock's wet heat conductivity.

Injection rate

Keeping all other parameters constant, the injection rate was changed from 100 cc/min to 10 cc/min and 1 cc/min, to evaluate influence on produced water temperature. The results are shown in Figure 11, and clearly indicate that by decreasing the water injection rate, the produced water's temperature increases. For example, by injecting 1 cc/min of 23 ^oC water into the rock sample, 1 cc/min of ~ 95 ^oC water will be produced, while injecting 10 cc/min of cold water produces 66 ^oC water.

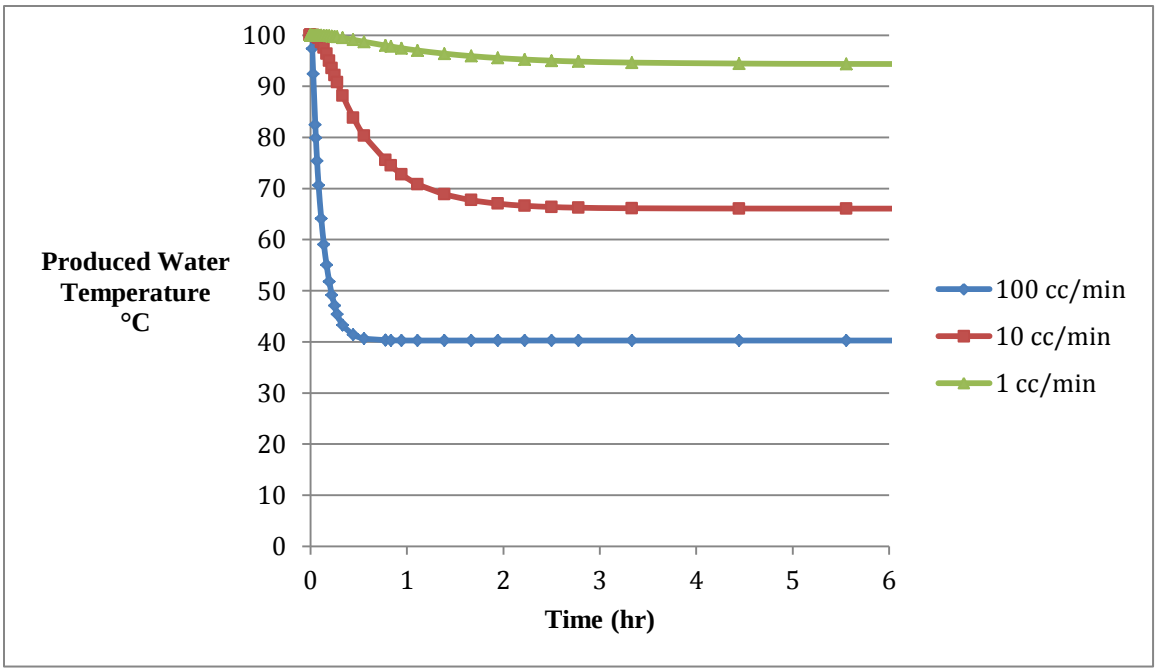

Figure 11. Effect of injection rate change on temperature of the produced water.

Rock Permeability

Next we consider how rock permeability can affect the production temperature. All other parameters were kept constant and the permeability value was changed from 750 mD to 75 mD and 7.5 mD. The simulations demonstrate that permeability does not influence steady state production well temperature, for the assumed boundary conditions at the wells (constant rate at injection well, constant pressure at producing well, and constant boundary temperature). But as indicated in Figure 12, it increases the injection pressure significantly at any given flow rate. In other words, compared to low permeability rocks, higher rock permeability allows for injection of more fluid at lower pressure, reducing risk of hydraulically fracturing the injected zone.

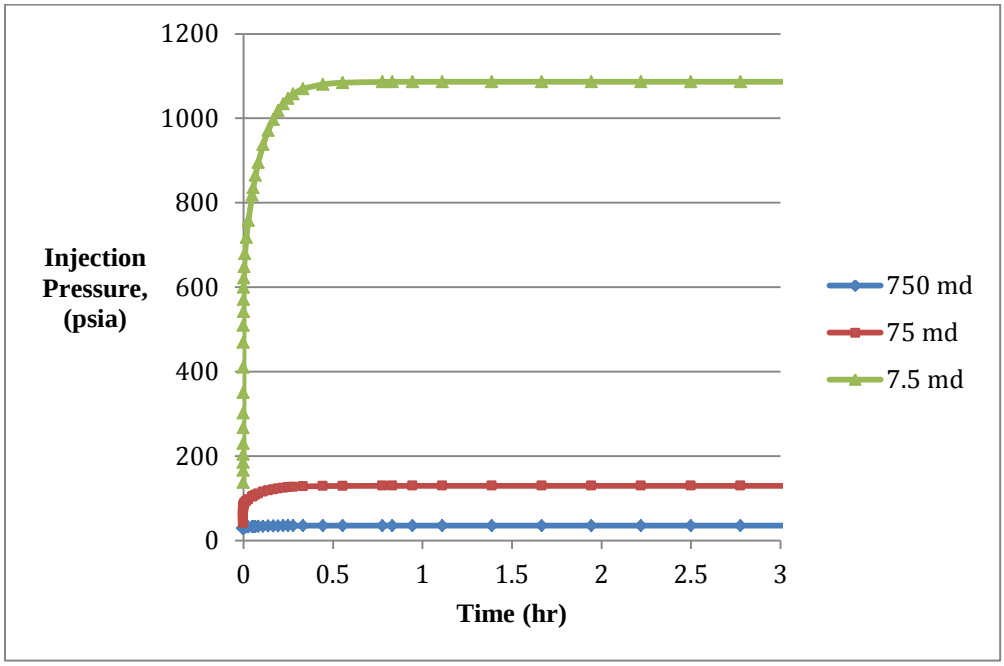

Figure 12. Influence of rock permeability on injection pressure, assuming 100 cc/min water injection.

Porosity, Specific Heat, and Rock Conductivity

To evaluate the effects of rock porosity on steady-state production temperature and injection pressure, all other parameters were kept constant and rock porosity was changed from 28% to 18% and 8%. There was no significant change in temperature and pressure results from this variation.

Specific heat is defined as the amount of heat required to raise the temperature of a 1 kg of a rock by 1^{o}c. In this study, a specific heat of 1000 J/Kg-C was used as the base number and then we considered additional specific heat values of 800 and 1200 J/kg-c in sensitivity analysis. There was no significant change in steady-state temperature and pressure results from this variation.

Thermal conductivity is a property of a material's ability to conduct heat. In this study, wet heat conductivity of 2 W/m-C was chosen for the base case and then varied to 1 and 4 W/m/C. The results of the sensitivity analysis demonstrate that heat conductivity coefficient has an important effect on heat exchange of the system and can influence the production temperature moderately. By increasing wet heat conductivity coefficient, the steady-state production temperature increases slightly and the injection pressure decreases slightly.

A summary of these sensitivity analyses is presented in Table 4, indicating the relative influence of each parameter on steady-state production temperature. We also repeated these sensitivity studies changing the base injection rate to 10cc/min. The relative influence of parameters on steady state production temperature did not change, although the final absolute values of temperature all increased. Finally we repeated the sensitivity studies changing the base permeability to 75md. Again the relative influence of parameters on steady state production temperature remained unchanged, although the absolute value of the injection pressure increased.

Table 4. Five key parameters used for sensitivity analysis and their values in the numerical model. Sensitivity of steady state production temperature to parameter variation provided in last two columns. The default injection rate is 100 cc/min.

Parameter	Value	Inj. Rate, cc/min	Perm., mD	Porosity, fraction	Wet Heat Cond, W/m-C	Specific Heat, J/kg-C	Production Temperature, °C	Importance, High/Low/ Moderate
Injection Rate, cc/min	100		750	0.28	2	1000	40	H
	10						66	
	1						94	
Permeability, mD	750	100		0.28	2	1000	40	L
	75						40	
	7.5						40	
Porosity	0.28	100	750		2	1000	40	L
	0.18						40	
	0.08						40	
Wet Heat Cond, W/m-°C	1	100	750	0.28		1000	36	M
	2						40	
	4						45	
Specific Heat, J/kg-C	800	100	750	0.28	2		40	L
	1000						40	
	1200						40	

6. Comparison to Laboratory Experiments

The laboratory experiments included three different tests with slightly different confining pressures (10, 25 and 50 psi). This was done to check for the accuracy of the results and the possibility of leakage in the system, but did not affect the permeability results significantly.

Using the injection rates, temperature and pressure settings from the laboratory experiment, we found the best permeability values which create the same differential pressure between the injection and production lines. Table 5 shows the differential pressure calculated numerically (in red color) versus lab results at three confining pressures of 10, 25 and 50 psi.

Table 5. Comparison between differential pressures measured by UCI and the numerical model of Terralog assuming 1140 md rock permeability. UCI carried out their measurements at three different confining pressures of 10, 25 and 50 psi.

Flow Rate [ml/min]	ΔP [psi] numerical	ΔP [psi] {Pc = 50}	ΔP [psi] {Pc = 25}	ΔP [psi] {Pc = 10}
2	0.17	0.19	0.24	0.22
5	0.41	0.41	0.44	0.48
10	0.84	0.84	0.86	0.89
15	1.25	N/A	1.29	1.3
20	1.65	1.62	1.67	1.68
25	2.03	N/A	N/A	2.08

With an assumed permeability of 1140md, we next applied the numerical model to simulate the observed temperature change in the laboratory experiments during sequential stepping of the injection rate. We present in the Figure 13 comparison of numerical simulations with laboratory results, for varying assumptions for rock conductivity. A reasonable match is achieved for a conductivity of about 3.7 W/m-C. The match is poorest for the lowest injection rate, but the simulated change in temperature versus time for subsequent higher injection rates are consistent with laboratory observations.

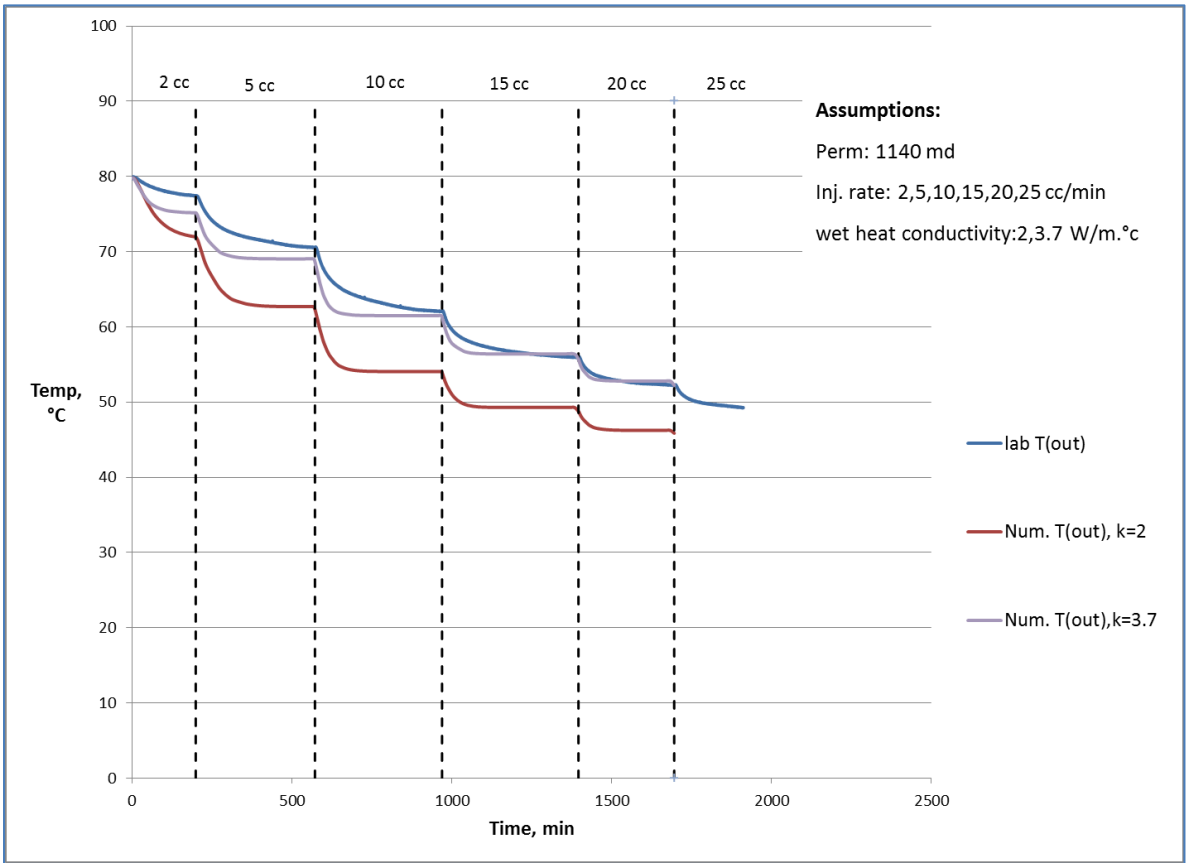

Figure 13. Comparison between numerical model and laboratory results at 90C for varying rock conductivity values.

7. Preliminary Conclusions and Discussion

We have initiated investigations into an innovative application of paired horizontal wells to establish a relatively closed-loop recirculation system for geothermal heat recovery in hot sedimentary rock. This investigation includes 1) Resource identification; 2) Laboratory investigations; 3) Laboratory and field scale numerical simulations; and, 4) Engineering feasibility and economic evaluation studies. We are currently in first year of a three year research project funded by the US Department of Energy, Geothermal Technologies Program. To date, we have completed assembly of laboratory equipment to investigate two dimensional flow in rock slab material, simulating the cross section perpendicular to two horizontal wells. We have initiated fluid flow and heat transfer experiments with water. We have developed a numerical simulation model which provides a reasonable match to laboratory observations.

During the next two years of the project we intend to further characterize hot sedimentary basins in the US which would be most appropriate for this technology. We will expand our laboratory equipment and experimentation to larger scale to investigate 3D flow and heat transfer. Finally we will complete detailed engineering feasibility and economic analyses to further evaluate and optimize the design of horizontal well pairs for geothermal energy recovery. The ultimate objective is to demonstrate the technical and economic viability of this technique to produce geothermal energy from previously untapped resources throughout the US.

References:

Holbrook, J., et al. "Tracking an energy elephant: Science and engineering challenges for unlocking the geothermal potential of sedimentary basins." *NSF workshop: Geothermal potential of sedimentary basins*. Salt Lake City, 2011.

Morgan, P., Sares, M. A., 2011, New horizons for geothermal energy in sedimentary basins in Colorado, Colorado Geological Survey, AAPG Search and Discovery Article #90124

Porro, C., Augustine, C., 2012, Estimate of geothermal energy resource in major U.S. sedimentary basins, National Renewable Energy Lab, Golden, Colorado, US Department of Energy

Pruess, K.,Oldenburg C., and Moridis G. (1999). TOUGH2 User's Guide, Lawrence Berkeley National Laboratory Report LBNL-43134, Berkeley CA.